Structural-Physiological Relationships in the Visual System upon Glutamate Excitotoxicity in the Eye using Diffusion Tensor Imaging and Manganese-enhanced MRI

Leon C. Ho[1,2], Bo Wang[3,4], Ian P. Conner[3,4], Yolandi van der Merwe[1,4], Richard A. Bilonick[3], Ed X. Wu[2], Seong-Gi Kim[1,5], Gadi Wollstein[3], Joel S. Schuman[3,4], and Kevin C. Chan[1,3]

[1]*Neuroimaging Laboratory, University of Pittsburgh, Pittsburgh, Pennsylvania, United States,* [2]*Department of Electrical and Electronic Engineering, The University of Hong Kong, Pokfulam, Hong Kong, China,* [3]*Department of Ophthalmology, School of Medicine, University of Pittsburgh, Pittsburgh, Pennsylvania, United States,* [4]*Department of Bioengineering, Swanson School of Engineering, University of Pittsburgh, Pittsburgh, Pennsylvania, United States,* [5]*Center for Neuroscience Imaging Research, Institute for Basic Science, Sungkyunkwan University, Suwon, Korea*

Target Audience: Basic and clinician scientists with interest in the structural and physiological properties in the distal neural pathways of the visual system upon excitotoxic injury to the proximal visual pathway in the eye.

Purpose: Excitotoxicity has been linked to the pathogenesis of ocular diseases and injuries such as retinal ischemia, traumatic injuries and glaucoma, and may involve early degeneration of both anterior and posterior visual pathways. To date, the spatiotemporal patterns of neurodegenerative events in the visual system and the relationships with excitotoxic retinal injury and optic neuropathy have not been fully elucidated. Here, we quantified *in vivo* the spatiotemporal profiles of microstructural alterations in the distal neural pathways of the mouse visual system upon N-methyl-D-aspartate (NMDA)-induced glutamate excitotoxicity in the eye with diffusion tensor imaging (DTI). In addition, manganese-enhanced MRI (MEMRI) of anterograde Mn transport along the visual pathway was performed to correlate between structural and physiological characteristics in the injured visual system.

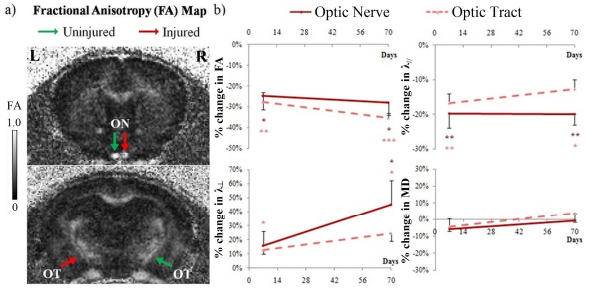

Figure 1. a) Representative FA maps of the optic nerve (ON) and optic tract (OT) at 7 days post-NMDA injury to the right eye. b) Spatiotemporal changes in DTI quantitation (mean ± standard error) in the injured optic nerve and injured optic tract relative to the uninjured visual pathway at 7 and 70 days post-NMDA injury. (Two-tailed paired t-tests between injured and uninjured visual pathways: *p<0.05, **p<0.01, ***p<0.001)

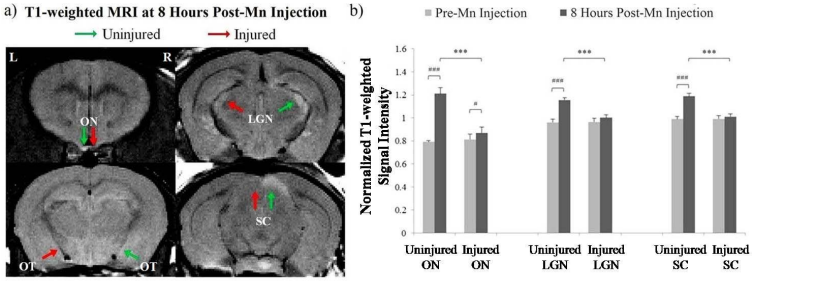

Figure 2. a) Representative T1-weighted images in the ON, OT, lateral geniculate nucleus (LGN) and superior colliculus (SC) at 7 days post-NMDA injury to the right eye and 8 hours post-Mn injection to both eyes. b) Quantitation of normalized T1-weighted signal intensities (mean ± standard error) of the mouse ON, LGN and SC at 7 days post-NMDA injection to the right eye, and before and 8 hours after intravitreal Mn injection to both eyes. Two-tailed paired t-tests between (i) injured and uninjured visual pathways *p<0.05, **p<0.01, ***p<0.001; (ii) pre-Mn injection and 8 hours post-Mn injection #p<0.05, ###p<0.001.

Methods: ***Animal Preparation:*** 6 adult C57BL/6 mice were intravitreally injected with 1μL of 40mM NMDA to the right eye to induce glutamate excitotoxicity. DTI was performed to the brain's visual system at 7 and 70 days after excitotoxic retinal injury. $MnCl_2$ solution (0.5μL of 100mM) was intravitraelly injected to both eyes right after DTI experiment at 7 days after NMDA injection, and MEMRI was performed at 8 hours after Mn administration. ***MRI Protocol:*** All scans were performed under isoflurane anaesthesia using a 9.4-Tesla/31-cm Varian/Agilent horizontal bore scanner with a 32mm transmit-receive volume coil. DTI was acquired using a fast spin echo sequence, with 2 non-diffusion-weighted b0 images and diffusion weighting at 12 diffusion gradient directions at b=1000s/mm^2. Other imaging parameters included: TR/TE=2300ms/27.8ms, ETL=8, δ/Δ=5/17ms, in-plane resolution=104x104μm^2 and slice thickness=0.5mm. Slices were oriented orthogonal to the prechiasmatic optic nerves. MEMRI was performed with a T1-weighted fast spin echo sequence using the same geometry as DTI, with TR/TE=1060ms/9.35ms, ETL=4. Co-registration between b0 and diffusion-weighted images were performed using SPM8. DTI paramatric maps including fractional anisotropy (FA), axial diffusivity ($\lambda_{//}$), radial diffusivity ($\lambda_{\perp}$) and mean diffusivity (MD) maps were computed using DTIStudio. Regions of interest (ROI) were manually drawn on the optic nerve (ON) and optic tract (OT) based on FA, $\lambda_{//}$, $\lambda_{\perp}$ maps. For MEMRI, ROIs were manually drawn on the ON, lateral geniculate nucleus (LGN) and superior colliculus (SC) based on T1-weighted images before and after Mn injection. MEMRI signal was normalized to the signal of a nearby saline phantom. A linear mixed-effects model was used to determine the effects of DTI microstructural changes in the ON on the anterograde Mn transport in ON, LGN and SC.

Results: Figs. 1a and 2a show lower FA and Mn enhancement along the posterior visual pathway projected from NMDA-injured right eye at 1 week post-NMDA injection compared to the uninjured visual pathway. Significant decrease in FA and $\lambda_{//}$ and significant increase in $\lambda_{\perp}$ were observed along the injured ON and injured OT at 7 to 70 days after NMDA-induced retinal injury (Fig. 1b). The highest rate of $\lambda_{//}$ decrease occurred within the 1st week post-NMDA injection, whereas $\lambda_{\perp}$ increase appeared to progress further after 1 week post-NMDA injection. At 1 week post-NMDA injection, significant Mn enhancement was detected along the uninjured visual pathway and in the injured ON but not the injured LGN or SC at 8 hours post-Mn injection compared to pre-Mn injection (Fig. 2b). In Figure 3, FA and $\lambda_{//}$ in ON were significantly correlated with relative Mn signal increase in ON, LGN and SC at 8 hours post-Mn injection to both eyes and 1 week post-NMDA injection to right eye.

Discussion: Excess NMDA level in the eye can induce early glutamate excitotoxic injury to the retinal and the central visual pathway dose-dependently [1]. Our DTI findings of the early $\lambda_{//}$ decrease and continual $\lambda_{\perp}$ increase in the ON within experimental period may reflect different progression rates for several neurodegenerative events known to occur in distal neural pathways such as early axonal injury and delayed demyelination [2]. In this study, the strong preferential correlations of Mn enhancement in the posterior visual pathways with FA and $\lambda_{//}$ but not $\lambda_{\perp}$ in the ON suggested the potential linkage between anterograde Mn transport disruption and compromised microstructures that predominated water diffusion changes parallel to the optic nerve such as microtubule and neurofilament injuries [3, 4].

Conclusion: The directional diffusivities $\lambda_{//}$ and $\lambda_{\perp}$ along the posterior visual pathway decreased and increased respectively at different progression rates after excitotoxic retinal injury. In addition, the preferential influence of reduced anterograde Mn transport by $\lambda_{//}$ but not $\lambda_{\perp}$ in the neural pathway may shed light on the microstructural basis of Mn transport mechanisms.

References [1] Lam T.T., Inves Ophthalmol Vis Sci., 1999; [2] Saggu S.K., BMC neuroscience, 2010; [3] You Y., PloS one, 2012; [4] Chan K.C., Neuroimage, 2008;

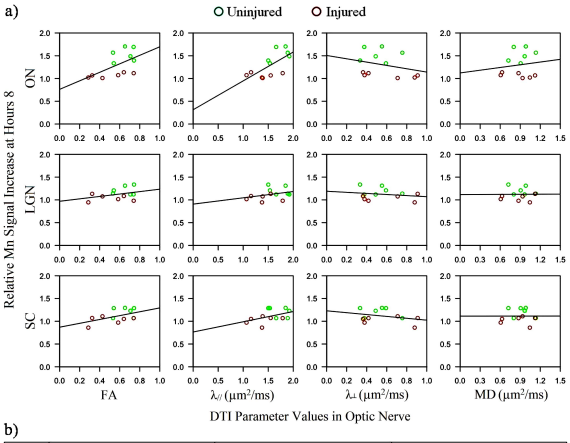

b)

Optic Nerve	ON - MEMRI			LGN - MEMRI			SC - MEMRI		
	Estimated Slope	Standard Error	P-value	Estimated Slope	Standard Error	P-value	Estimated Slope	Standard Error	P-value
FA	0.350	0.079	**0.007**	0.774	0.277	**0.032**	0.752	0.233	**0.023**
λ||	0.729	0.126	**0.002**	1.617	0.484	**0.021**	1.411	0.453	**0.026**
λ⊥	-0.225	0.114	0.104	-0.521	0.325	0.582	-0.542	0.277	0.108
MD	0.093	0.101	0.397	0.209	0.271	**0.001**	0.143	0.251	0.594

Figure 3. a) Scatter plots of the relationships between DTI parameters in ON and relative Mn signal increases in ON, LGN and SC at 1 week post-NMDA injury. The black line corresponds to a simple linear regression. b) The estimated slopes of the corresponding scatter plots after accounting for the use of both eyes (p<0.05: estimated slopes are significantly different from 0).